Biosensors and Bioelectronics 81 (2016) 151–158

Contents lists available at ScienceDirect

Biosensors and Bioelectronics

journal homepage: www.elsevier.com/locate/bios

Label-free in-situ real-time DNA hybridization kinetics detection employing microfiber-assisted Mach-Zehnder interferometer

Binbin Song, Hao Zhang *, Bo Liu, Wei Lin, Jixuan Wu

Key Laboratory of Optical Information Science and Technology, Ministry of Education, Institute of Modern Optics, Nankai University, Tianjin 300071, China

ARTICLE INFO

Article history:
Received 18 December 2015
Received in revised form
24 February 2016
Accepted 25 February 2016
Available online 27 February 2016

Keywords:
Microfiber
Mach-Zehnder interferometer
DNA hybridization
Microcavity

ABSTRACT

A label-free DNA biosensor based on microfiber-assisted Mach-Zehnder interferometer (MAMZI) for in-situ real-time DNA hybridization kinetics detection has been proposed and experimentally demonstrated. A microfiber of hundreds of microns in length is fabricated by tapering a segment of standard single-mode fiber (SMF) to construct the U-shaped microcavity between the lead-in and lead-out SMFs. Thanks to the mode field mismatching between the SMF and microfiber, the incident guided mode light would separate into two beams that respectively propagate in the air microcavity and the microfiber. Consequently, interference between different light modes would occur at the joint between the microfiber and the lead-out SMF. Experimental results indicate that owing to the participation of opening cavity modes in the modal interference process, the interferometric spectrum of our proposed microcavity sensor is highly sensitive to the variation of environmental refractive index (RI), especially for the RI range around 1.34 which is useful for most biological applications. The microfiber functionalization is achieved by stepwise modifying the microfiber with monolayer Poly-L-lysine (PLL) and single-stranded DNA (ssDNA) probes to produce the sensitive surface that could uniquely attach specific target ssDNAs. The fiber surface functionalization as well as DNA hybridization processes have been experimentally investigated for different target ssDNA solutions in real time. The interferometric transmission spectrum shows large wavelength shift for different biological phases, and a detection limit conservatively down to 0.0001 pmol/μL has been acquired by employing the U-shaped microcavity of 176.88 μm in length. Our proposed DNA biosensor possesses several advantages such as compact size, ease of fabrication, and strong response for DNA hybridization, which make it a promising candidate for potential applications in such rapidly expanding areas as medical diagnosis, cancer screenings, medicine examination and environmental engineering, etc.

1. Introduction

In the past decade, in-situ detection of DNA hybridization has been extensively investigated due to the ever-growing demand for specific recognition of DNA sequence in the fields of genetic study (Kleinjung et al., 1997), medical diagnostics (Schmidt et al., 2002), environmental science and biological engineering (Candiani et al., 2013). Amongst different DNA detection techniques, optical interrogation is one of the most widely investigated transduction approach (Fan et al., 2008; Endo et al., 2010; Viphavakit et al., 2015). A great mount of current DNA detection schemes depend on fluorescence as the transition signal (Long et al., 2011; Coscelli et al., 2010). However, it is normally required to label fluorescent groups on target DNA, which not only complicates the functionalization process but also increase the fabrication cost. Besides, since high performance excitation light sources and fluorescence detectors are also indispensable, it would be rather difficult to realize real-time detection of DNA hybridization process. Actually, label-free detection devices for real-time and in-situ detection of DNA hybridization have been widely studied for the past few years. In particular, fiber-sensor-based label-free detection of DNA hybridization offers such desirable merits as compactness, structural flexibility, ease of remote control for in-situ detection occasions, rapid response and high sensitivity for target molecules in real time (Chryssis et al., 2005; Rindorf and Jensen, 2006; Leung et al., 2008; Herath et al., 2011; Delport et al., 2012; Sun et al., 2014; Liu et al., 2015).

A good variety of label-free DNA detection schemes have been proposed by utilizing *evanescent-field-based fiber-optic devices. Particularly, microfibers have been widely employed as one kind of typical structure to excite evanescent field for investigation of* the interaction between excitation light and DNA molecules (Chryssis et al., 2005; Herath et al., 2011; Sun et al., 2014). However, evanescent wave normally only exists very close to the microfiber

* Corresponding author.
E-mail address: haozhang@nankai.edu.cn (H. Zhang).

http://dx.doi.org/10.1016/j.bios.2016.02.065
0956-5663/

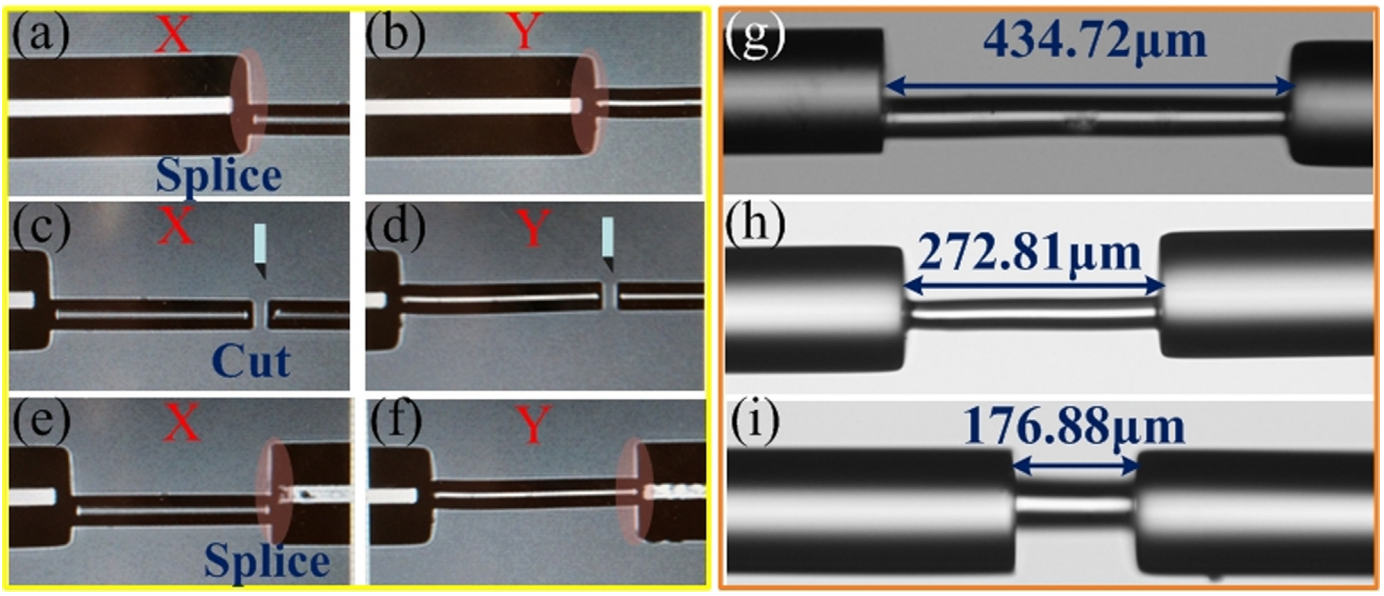

Fig. 1. Micrographs of the MAMZI fabrication procedure (a)–(f); the U-shaped microcavities of (g) 434.72 μm, (h) 272.81 μm and (i) 176.88 μm in length, respectively.

surface with about 100 nm in depth and would exponentially decay as it propagates along the fiber axis, which makes it unavailable for detection of the bio-analyte a bit farther away from the fiber surface. *It should be noted that surface-plasmon-resonance-based (SPR-based) evanescent field enhancement schemes have attracted increasing research interests in recent years* (Leung et al., 2008; Delport et al., 2009, 2012; Verma and Gupta, 2013). *However, the SPR performances are dependent on metal thickness, functional layer configuration, and bio-molecular size. Since SPR effect is dominated by transverse magnetic (TM) waves that could only be excited by p-polarization light, special polarization light source is normally required to excite the SPR effect. Moreover, the quality of SPR signal is restricted by the strength of evanescent wave.* In this case, to lower the detection limit for DNA molecules by enhancing their interaction with the light field is an issue to be promptly resolved.

In general, two methods could be employed to improve the DNA sensitivity for fiber-optic label-free DNA detectors. One is to increase the length of transduction element, by which the fiber surface is enlarged to attach more bio-molecules. However, due to the increase of sensor size, point detection for microscale biosamples is not possible. The other method is to decrease fiber diameter to strengthen the microfiber evanescent field. This enhances the interaction between evanescent field and target biomolecules, but the microfiber is rather fragile and complex fabrication procedure is also required. Due to the drawbacks of current fiber-optic bio-sensor designs, it would be necessary to develop a fiber-optic bio-detector with such desirable features as compactness, low cost, robust, strong interaction between the evanescent field and biosamples and ease of integration with bio-molecules.

In this paper, a microfiber-assisted Mach-Zehnder interferometer (MAMZI) has been proposed for label-free detection of DNA hybridization in real time. A segment of microfiber is spliced between two standard single-mode fibers (SMFs) with large lateral offset to constitute an opening U-shaped cavity. The proposed biosensor has a miniaturized structure, and moreover about half of the incident light power is injected into the opening cavity to ensure strong interaction between the evanescent field and biosample. In 2013 we developed a microfiber-assisted U-shaped cavity with ultrahigh sensitivity for ambient RI around 1.34 (Gao et al., 2013), which exploits the enhanced interaction between light and ambient medium with the help of the opening U-shaped cavity. The good RI responses of this sensor provide the possibility of developing miniaturized biosensors with ultrahigh sensitivities for label-free detection of small bio-molecules. The U-shaped cavities of 434.72 μm, 272.81 μm and 176.88 μm in length were experimentally fabricated, and the microfiber surfaces were functionalized with a monolayer of poly-L-lysine (PLL) and a single-stranded DNA (ssDNA) probe. Both of the surface functionalization and DNA hybridization processes have been experimentally investigated in real time. With the same surface functionalization procedure, strong responses of interferometric spectrum have been acquired for DNA hybridization kinetics characterization. And to the best of our knowledge, our proposed DNA detector has the smallest size compared with the ever reported designs (Chryssis et al., 2005; Rindorf and Jensen, 2006; Leung et al., 2008; Herath et al., 2011; Delport et al., 2009, 2012; Verma and Gupta, 2013; Sun et al., 2014; Liu et al., 2015).

2. Microfiber-assisted MZI

2.1. Fabrication of U-shaped cavity

The MAMZI is fabricated by using a commercial fusion splicer (Fujikura FSM-60s, Japan). The micrographs of the device fabrication procedure are shown in Fig. 1. Firstly, the cladding diameter of a segment of SMF (SMF-28e, Corning Inc., USA) is tapered down to tens of microns based on flame scanning tapering technique. The uniform microfiber is spliced with a standard SMF with a large lateral offset along *X* direction but laterally aligned along *Y* direction to constitute one of the interferometric arms, as shown in Fig. 1(a) and (b), respectively. By using a translation stage to accurately adjust the fiber axial displacement and a fiber cleaver to cut off the free end of the microfiber, the microfiber with predesigned length could be fabricated, as shown in Fig. 1(c), (d) respectively. After the microfiber is cut off, it is spliced with the lead-out SMF, as shown in Fig. 1(e) and (f), respectively. By repeating the above procedure, three MAMZIs with cavity lengths of 434.72 μm, 272.81 μm and 176.88 μm were fabricated, as shown in Fig. 1(g)–(i), respectively. Compared with related reports on fiber-optic DNA detectors, our proposed DNA biosensor has the most compact structure (Chryssis et al., 2005; Rindorf and Jensen, 2006; Leung et al., 2008; Herath et al., 2011; Delport et al., 2009,

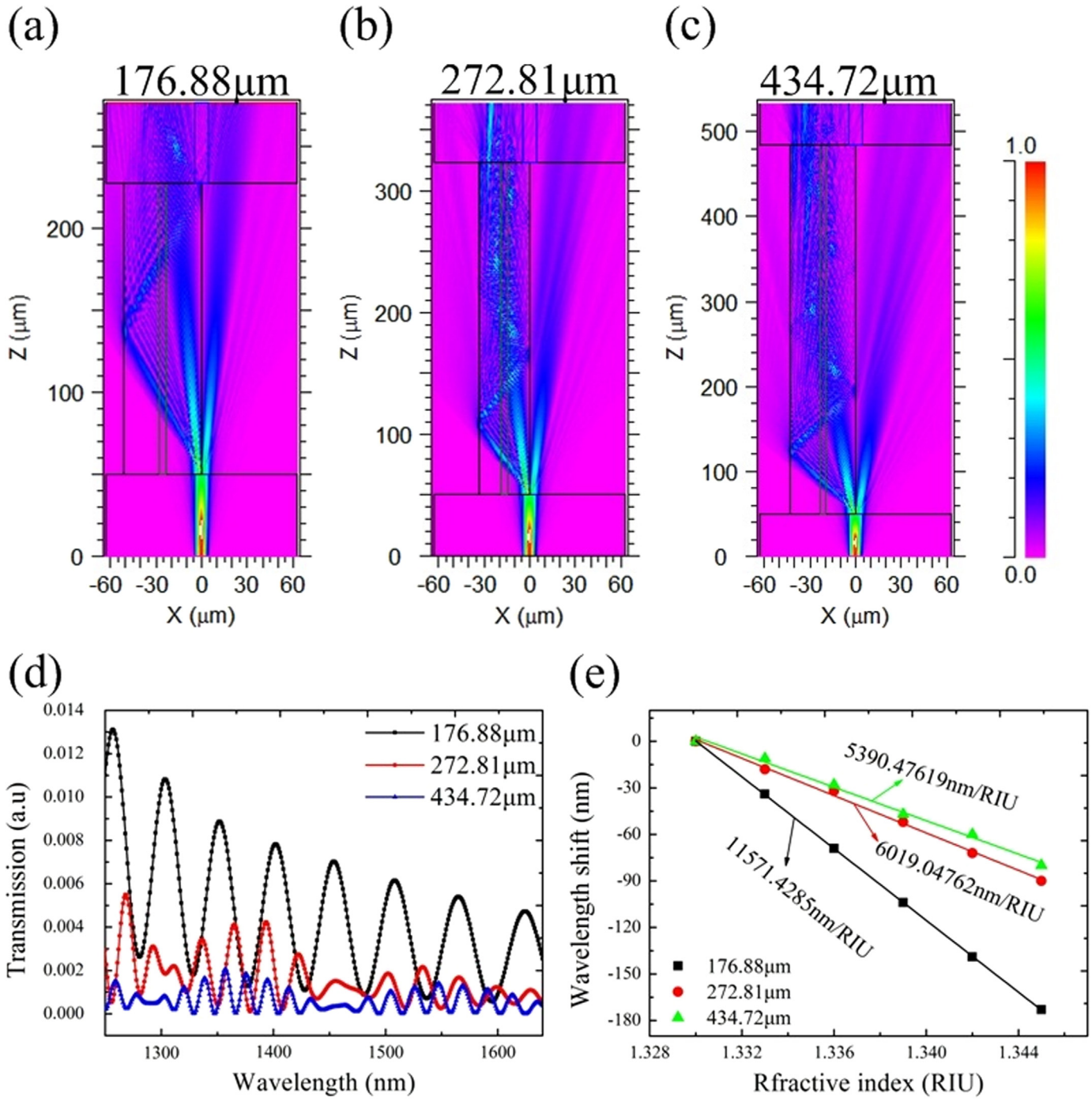

Fig. 2. Simulation of beam propagation process for the MAMZIs with different microcavity lengths (a)–(c); (d). Simulated transmission spectra; (e). Wavelength shift in response to the change of ambient RI around 1.34.

2012; Verma and Gupta, 2013; Sun et al., 2014; Liu et al., 2015).

2.2. Performances of the microfiber-assisted MZI

2.2.1. The beam propagation mechanism

Due to the presence of large lateral offset between the lead-in SMF and microfiber, as incident guided core mode from the lead-in SMF enters the microcavity region it would separate into two different branches that propagate along the microfiber and U-shaped cavity, respectively. And owing to the mode field mismatching between the microfiber and lead-out SMF, the two beams respectively propagating along the U-shaped cavity and microfiber would interfere at the joint between the microfiber and lead-out SMF. Based on the beam propagation theory, the power evolution process as the light propagates through the MZI structure has been simulated for the above three MAMZIs, as illustrated in Fig. 2(a)–(c), respectively. It is apparent that the incident light generally splits into two portions, and nearly half of the incident light leaks into the air environment. Due to the optical path difference between these two portions of light, spectral interference would occur at the joint between the microfiber and lead-out SMF.

Simulated transmission spectra for the MAMZI with different microcavity lengths in air are illustrated in Fig. 2(d). It could be seen that due to the scattering of air, the microcavity with longer cavity length would experience larger transmission loss. Different from the one of 176.88 μm in length, the interferometric

transmission spectra exhibit a few irregular fluctuations for the U-shaped cavities of 272.81 μm and 434.72 μm in length. This is due to the fact that as the length of microcavity increases, interference may take place between the guided modes propagating in the microfiber and U-shaped cavity before they meet at the output of the microfiber, which results in the superposition of multiple interferences. The decrease of microfiber length would help to suppress the superposition of multiple interferences. As the length of U-shaped cavity is shortened to 176.88 μm, the interferometric transmission spectrum with lowest transmission loss and highest contrast may be acquired, which could be simulated using a rigorous double-beam interference model.

2.2.2. Theoretical evaluation of RI sensing performances

To evaluate the sensing performances for the low RI range around 1.34, we have simulated the transmission dip wavelength shift as the ambient RI of the proposed MAMZIs with different cavity lengths ranges from 1.33 to 1.345, as shown in Fig. 2(e). From this figure, it is clear that the interference dips linearly move toward shorter wavelength region as the ambient RI increases. The spectral blue-shift is caused by the decrease of optical path difference between the guided modes propagating in the microfiber and U-shaped cavity as the RI of the U-shaped cavity increases. Simulation results indicate that the RI sensing sensitivities as large as 5.3905×10^3 nm/RIU, 6.019×10^3 nm/RIU and 1.15714×10^4 nm/RIU could be obtained for the MAMZIs with U-shaped cavities of 434.72 μm, 272.81 μm and 176.88 μm in length, respectively; and the lowest RI detection limit reaches 4.32×10^{-5} RIU in consideration of the 0.5 nm wavelength resolution of the optical spectrum analyzer (OSA) employed in our experiment.

3. DNA hybridization detection

3.1. Surface functionalization of the microfiber

3.1.1. Reagent

Poly-L-lysine (PLL) (Sigma, molecular weight: 30000–70000); PBS buffer (0.01 mol Na2HPO4, 0.15 mol NaCl, pH=7.4); TE buffer (10 mmol Tris–HCl 1 mmol EDTA pH=7.4); Ultrapure water; Methylene Blue (MB) ($C_{16}H_{18}ClN_3S \cdot 3H_2O$, molecular weight: 373.9); Probe ssDNA: 5′-AAG CTT CGC TGA GGA ACA CAT-3′; and its matched target ssDNA: 5′-ATG TGT TCC TCA GCG AAG CTT-3′; *non-complementary* ssDNA: 5′-GCC AAC AGG GAG AAG ATG ACC-3′.

The PBS buffer and TE buffer are sterilized under high temperature and high pressure, standby at 4 °C. 25 mg/ml PLL/PBS solution is prepared in 25 mg PLL and 1 mL PBS buffer, standby at −25 °C. Additional small concentrations are diluted in PBS buffer. The ssDNA *samples* are dissolved in 1 × TE buffer, respectively, and solutions with different concentrations of 1.0 pmol/μL, 0.5 pmol/μL, 0.2 pmol/μL, 0.1 pmol/μL, 0.05 pmol/μL, 0.02 pmol/μL, 0.01 pmol/μL, 0.005 pmol/μL, 0.002 pmol/μL, 0.001 pmol/μL, and 0.0001 pmol/μL are prepared, standby at 4 °C.

3.1.2. Surface functionalization

Silica surface of the microfiber is inherently negatively charged (He et al., 2011). PLL is commonly used to immobilize negatively charged biomolecules (such as DNA) on the surface of solid substrate. PLL has amino-groups with positive charges that could be bound to the negatively charged microfiber surface through ionic absorption (Rindorf and Jensen, 2006). Thus the microfiber could be functionalized with a monolayer PLL. In addition, ssDNA has phosphate groups in its negatively charged backbone, which could be immobilized to the other end of monolayer PLL but would not be directly bound to the negatively charged fiber surface. As illustrated in Fig. 3(a), PLL and probe ssDNA immobilized on the microfiber surface would gradually form a sandwich-like coating surrounding the microfiber.

The functionalization procedure are stepwise illustrated in Fig. 3(b). Firstly, the microfiber is cleansed by ultrapure water through a micro-flow cell. And then the prepared 25 mg/mL PLL/PBS solution is diluted by 250 times and pumped into the U-shaped cavity for 1 h. The same cleansing procedure using ultrapure water is repeated twice to remove the non-immobilized PLL molecules. The ionic absorption-based monolayer PLL would form on the microfiber surface at this moment. 1 pmol/μL probe ssDNA/TE buffer is pumped into the U-shaped cavity for 1 h to ensure that ssDNA molecules are immobilized on the monolayer PLL. Then it is cleansed by ultrapure water to remove the non-immobilized probe ssDNA molecules. Following the above procedure, we could acquire a sandwich-like modification and functionalization structure with microfiber as the substrate material.

To prove the functionalization of the microfiber surface, Methylene Blue (MB) is used to dye double-stranded DNA (dsDNA), whose tricyclic heterocyclic molecular structure would intercalate between the basepairs of G–C of dsDNA (Muller and Crothers, 1975). Fig. 3(c) shows the side view micrographs of microfiber without surface functionalization after immersion into MB/water solution, no MB dye could be found on the microfiber surface. Its inset shows the micrograph of MB/water solution on a glass slide, on which rare MB dye aggregations could be found. In contrast, Fig. 3(d) shows the side view micrograph of the microfiber with surface functionalization and DNA hybridization after immersion into the MB/water solution. It is apparent that MB dye aggregates on the microfiber surface. The inset shows MB/water solution with dsDNA on a glass slide, on which MB dye aggregations could also be found.

3.2. Experimental setup of the DNA hybridization probe

Fig. 4 shows the schematic experiment setup of the DNA hybridization detection system. Our proposed MAMZI is encapsulated into a micro-flow cell with micro V-groove to serve as the DNA probe. All of the liquid samples are injected into the cell by using a syringe pump. Due to the teeny size of MAMZI, just submicroliter sample volumes (0.866 μL) should be pumped into the microcell. Light from a supercontinuum broadband source (SBS) is launched into the MAMZI and the interferometric transmission spectrum is monitored in real time during the surface modification and DNA detection procedures by employing an OSA (Yokogawa AQ6370C, operation wavelength ranges from 600 nm to 1700 nm) with a wavelength resolution of 0.5 nm.

4. Experimental results and discussion

4.1. Results of complementary DNA hybridization detection

Fig. 5 shows the transmission spectra as well as the real-time interference dip shift in response to PLL modification and DNA hybridization for the three MAMZIs with different microcavity lengths. The interferometric transmission spectra of the MAMZI with U-shaped cavities of 434.72 μm, 272.81 μm and 176.88 μm in length are shown in Fig. 5(a), (c) and (e), respectively. Due to the large cross sectional offset between the SMF and microfiber, about half of the total incident light enters the air cavity, causing a large transmission loss over 30 dB. When the MAMZIs are exposed in the air, the free spectral ranges (FSRs) of the interferometric transmission spectra located around 1550 nm are 11.7 nm, 19.0 nm and 29.7 nm, respectively. The FSR $\Delta\lambda$ could be roughly evaluated by $\Delta\lambda = \lambda^2/\Delta nL$, where λ represents the average transmission dip

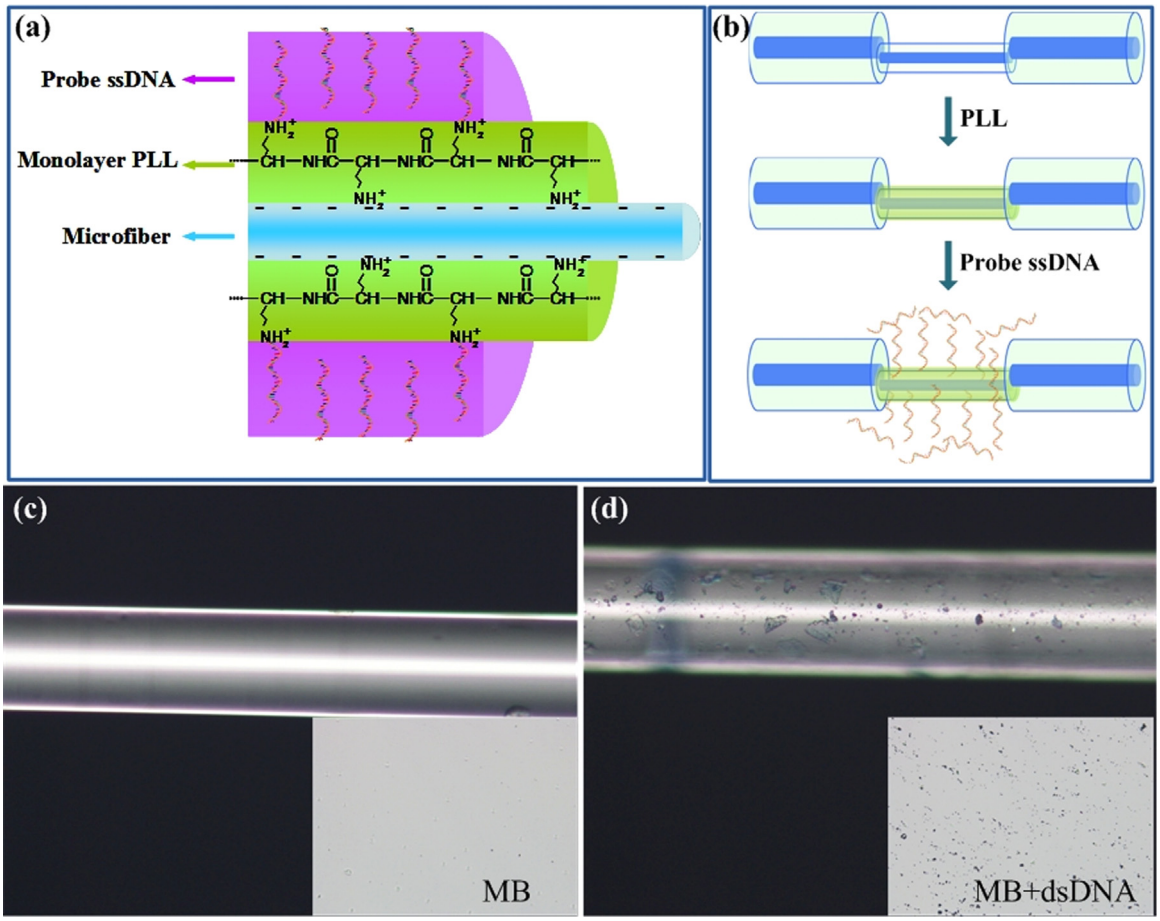

Fig. 3. (a) Schematic diagram of the sandwich-like modified and functionalized structure with microfiber as the substrate material. (b) Stepwise functionalization procedure. (c) Side view micrographs of microfiber without surface functionalization after immersion into the MB solution; inset shows the MB/water solution on a glass slide. (d) Microfiber with surface functionalization and DNA hybridization after immersion into the MB solution; Inset shows the MB/water solution with dsDNA on a glass slide.

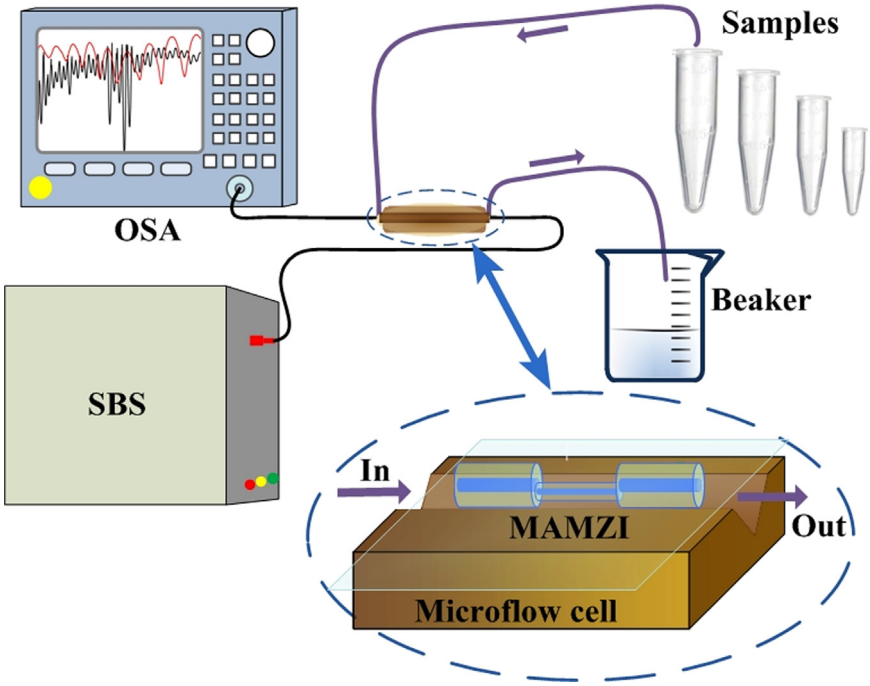

Fig. 4. Schematic experiment setup of the DNA detection system.

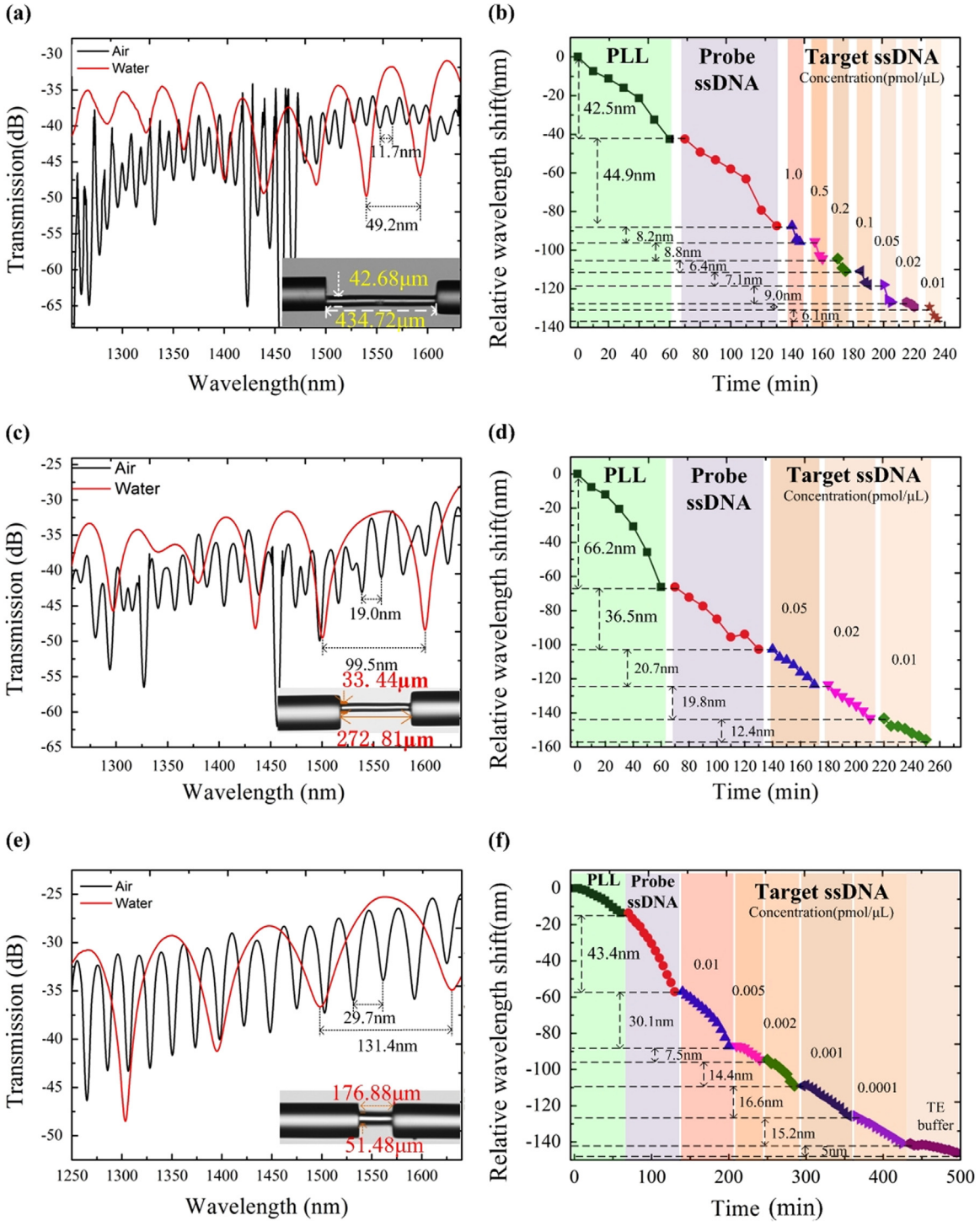

Fig. 5. Interference spectral responses. (a), (c) and (e) show interference spectra of the MAMZIs with U-shaped cavities of 434.72 μm, 272.81 μm and 176.88 μm in length, respectively. (b), (d) and (f) show the real-time relative wavelength shift responses of the MAMZIs to microfiber surface functionalization and DNA hybridization processes.

wavelength, Δn refers to RI difference between the optical modes participating in the modal interference process and L is interference length. For air environment, the RI difference around 1550 nm could be approximated by $\Delta n = n_s - 1 = 0.4635$, where n_s refers to RI of the silica-based microfiber. Therefore, the theoretically calculated FSRs for the above three MAMZIs with different cavity lengths are 11.92 nm, 18.99 nm and 29.3 nm respectively, which are in good agreement with our experimental results. When pure water is pumped into the microflow cell, transmission spectra with better periodic pattern could be obtained, as shown in Fig. 5(a), (c) and (e). This implies that fewer modes would participate in the modal interference process owing to the increment of microcavity RI. And due to decrease of the RI difference, the FSRs increase to 49.2 nm, 99.5 nm, 131.4 nm for different MAMZIs, respectively.

The transmission spectral responses have been monitored in real-time for microfiber surface modification and functionalization processes as well as the detection process for target ssDNA with different concentrations. Fig. 5(b), (d) and (f) give the interference dip responses for different biological phases. 0.1 mg/mL PLL/PBS

solution is in turn pumped into the microcavities of 434.72 μm and 272.81 μm in length. Due to the ionic absorption effect between the microfiber and PLL amino groups, the interference spectra exhibit large wavelength shifts of 42.5 nm and 66.2 nm after an observation time span of 1 h, respectively. This indicates that our proposed MAMZIs possess ultrahigh wavelength sensitivity to PLL molecules. For the microcavity of 176.88 μm in length, after diluting the 0.1 mg/mL PLL/PBS solution by 100 times by using PBS buffer, it is also pumped into the microflow cell for 1 h. And this time a wavelength shift of 13.6 nm has been experimentally acquired. And when 1 pmol/μL probe ssDNAs are pumped into the above three U-shaped cavities for 1 h, strong absorption interaction between monolayer PLL and phosphate groups of probe ssDNA molecules results in obvious wavelength shifts up to 44.9 nm, 36.9 nm and 43.4 nm, respectively.

After immobilization of probe ssDNA molecules on the microfiber surface, the complete complementary ssDNA sequence with different concentrations as target ssDNA are respectively pumped into the microflow cell. For the U-shaped cavity of 434.72 μm in length, a series of target ssDNA concentrations of 1.0 pmol/μL, 0.5 pmol/μL, 0.2 pmol/μL, 0.1 pmol/μL, 0.05 pmol/μL, 0.02 pmol/μL and 0.01 pmol/μL are selected for experimental test. Owing to the complementary base pairing action, even for the case of 0.01 pmol/μL, an evident wavelength shift of 6.1 nm has been acquired in only 5 min. In this case target ssDNAs with lower concentrations of 0.05 pmol/μL, 0.02 pmol/μL and 0.01 pmol/μL are respectively pumped into the microflow cell when the U-shaped cavity of 272.81 μm in length is employed. In half an hour, the wavelength shifts decrease from 20.7 nm to 12.4 nm for the target ssDNAs with different concentrations, which means that the detection limit of the proposed MAMZI for target ssDNA is even lower than 0.01 pmol/μL. To recognize the detection limit for DNA hybridization, target ssDNA samples with lower concentrations, including 0.005 pmol/μL, 0.002 pmol/μL, 0.001 pmol/μL, and 0.0001 pmol/μL, are in turn pumped into the 176.88 μm-microcavity. All of the low concentration samples show obvious wavelength shifts within an observation time span of 1 h, and even for the sample with lowest concentration (0.0001 pmol/μL), a wavelength shift of 15.2 nm has been acquired. To evaluate the influence of ionic electrostatic incorporation in TE buffer, the transmission spectrum has been also monitored for 1 h when TE buffer is applied only. The interference dip shows a slight wavelength shift by about 5 nm within 1 h, which is acceptable compared with the wavelength shifts of 15.2 nm when 0.0001 pmol/μL target ssDNA sample is tested. In addition, it could be seen that the detection limit of complete complementary target ssDNA is less than 0.0001 pmol/μL.

4.2. Detection of specificity and repeatability

To evaluate the specificity for hybridization between different ssDNA sequences, the control experiment for non-complementary ssDNA (5′-GCC AAC AGG GAG AAG ATG ACC-3′) has been conducted utilizing the MAMZI with a microcavity length of 272.81 μm, as shown in Fig. 6(a). The interferometric dip around 1370 nm exhibits different spectral responses for complementary and non-complementary ssDNA samples. For the complementary target ssDNA samples with concentrations of 0.01 pmol/μL and 0.02 pmol/μL, the dip around 1370 nm shows a blue-shift of 9.5 nm and 13.8 nm within an observation time of 30 min, respectively. While for the 1 pmol/μL non- complementary ssDNA sample, the same transmission dip only experiences a small wavelength fluctuation of 1.5 nm within 30 min, which is caused by the electrostatic adsorption between trivial unsaturated PLL molecules and the structural mismatch of ssDNA molecules. The strong contrast in dip wavelength sensitivities indicate that our proposed MAMZI-based DNA detector possesses a good specificity for DNA recognition.

After detecting each one-target ssDNA sample, the performance repeatability of the MAMZI functionalized by PLL and probe ssDNA is verified based on thermal method. Through heating the MAMZI with dsDNA at 95 °C for 5 min and then fast cooling it at 0 °C for 2 min, the double helix structure of the dsDNA would become unstable and unwound, and the interferometric transmission spectrum would restore to its original pattern. For the microfiber of 176.88 μm in length, three repeated tests for 0.01 pmol/μL target ssDNA samples are conducted in real time, as shown in Fig. 6(b). The same condition for microfiber surface modification and functionalization are pledged as above described. After thermally unwinding, the MAMZI is kept in pure water for 1 h so that its interferometric transmission spectrum is fairly stable with little fluctuations. The functionalized surface of microfiber is reusable but small memory effect is existent. The average wavelength shifts and relative standard deviation (RSD) are 24.7 nm and 18.9% respectively within a monitoring time span of 60 min as shown in the insert of Fig. 6(b). These results indicate that our proposed MAMZI shows good repeatability, which ensures its applicability for practical applications.

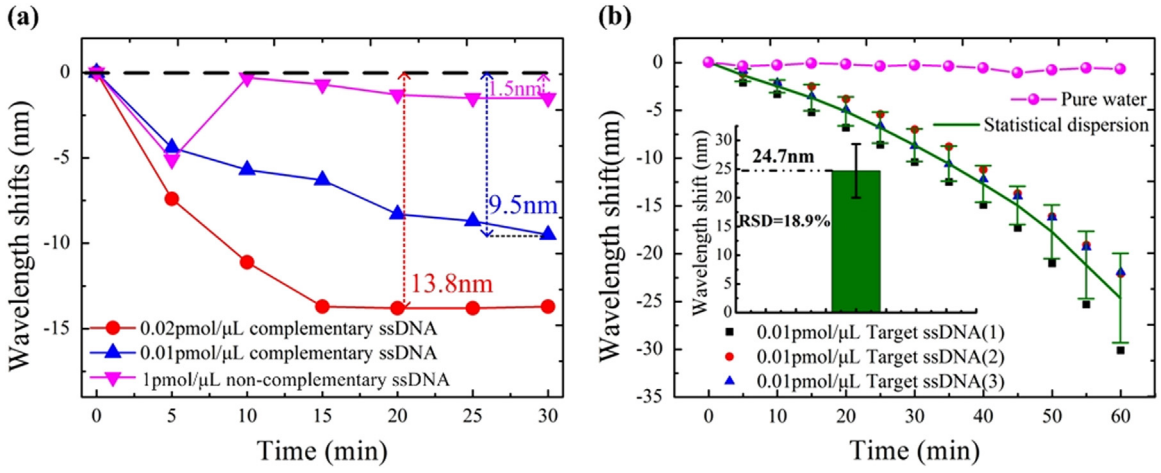

Fig. 6. (a) Control test for non-complementary ssDNA of the MAMZI with a microcavity length of 272.81 μm. (b) Repeatability test of the MAMZI with a microcavity length of 176.88 μm for 0.01 pmol/μL target ssDNA samples. Inset shows a histogram of the average wavelength shift within 60 min for three repeated tests; the error bars indicate the standard deviations at different time.

5. Conclusion

A label-free in-situ DNA hybridization kinetics probe based on a MAMZI has been proposed and experimentally demonstrated. The physical and bio-optic properties of the microcavities with different lengths have been investigated from theoretical as well as experimental perspectives. The stepwise modification and functionalization processes of the microfiber surface by employing monolayer PLL and ssDNA probe have been monitored in real time. For the shortest microcavity length of 176.88 μm, large wavelength shifts and an ultralow detection limit evaluated according to the experimental results is less than 0.0001 pmol/μL. In addition, the performance *specificity* and repeatability of the MAMZI functionalized by PLL and probe ssDNA has been tested. Our proposed MAMZI has the most compact structure and ultrahigh sensitive responses to DNA hybridization, which would be of great significance for the detection of trace biosamples and is anticipated to find various applications in the fields of medical diagnosis, cancer screenings and environmental engineering.

Acknowledgments

This work was jointly supported by the National Natural Science Foundation of China under Grant nos. 61377095 and 11274182, the 863 National High Technology Program of China under Grant no. 2013AA014201, and the Fundamental Research funds for the Central Universities.

References

Candiani, A., Bertucci, A., Giannetti, S., Konstantaki, M., Manicardi, A., Pissadakis, S., Cucinotta, A., Corradini, R., Selleri Label-free, S., 2013. DNA biosensor based on a peptide nucleic acid-functionalized microstructured optical fiber-Bragg grating. J.Biomed. Opt. 18 (5), 057004.

Coscelli, E., Sozzi, M., Poli, F., Passaro, D., Cucinotta, A., Selleri, S., Corradini, R., Marchelli Toward, R., 2010. A highly specific dna biosensor: PNA-modified suspended-core photonic crystal fibers. IEEE J. Sel. Top. Quantum Electron. 16 (4), 967–972.

Chryssis, A.N., Saini, S.S., Lee, S.M., Yi, H., Bentley, W.E., Dagenais, M., 2005. Detecting hybridization of DNA by highly sensitive evanescent field etched core fiber Bragg grating sensors. IEEE J. Sel. Top. Quantum Electron. 11 (4), 864–872.

Delport, F., Janssen, K.P.F., Jans, K., Maes, G., Pfeiffer, H., Wevers, M., Lammertyn, J., 2009. Fiber optic SPR biosensing of DNA hybridization and DNA–protein interactions. Biosens. Bioelectron. 25, 864–869.

Delport, F., Pollet, J., Janssen, K., Verbruggen, B., Knez, K., Spasic, D., Lammertyn, J., 2012. Real-time monitoring DNA hybridization and melting processes using a fiber optic sensor. Nanotechnology 23, 065503.

Endo, T., Ikeda, D., Kawakami, Y., Yanagida, Y., Hatsuzawa, T., 2010. Fabrication of core–shell structured nanoparticle layer substrate for excitation of localized surface plasmon resonance and its optical response for DNA in aqueous conditions. Anal. Chim. Acta 661, 200–205.

Fan, X.D., White, I.M., Shopova, S.I., Zhu, H.Y., Suter, J.D., Sun, Y.Z., 2008. Sensitive optical biosensors for unlabeled targets: a review. Anal. Chim. Acta. 620, 8–26.

Gao, S.C., Zhang, W.G., Bai, Z.Y., Zhang, H., Geng, P.C., Lin, W., Li Ultrasensitive, J.L., 2013. Refractive index sensor based on microfiber-assisted U-shape cavity. IEEE Photon. Technol. Lett. 25 (18), 1815–1818.

Herath, C., Wang, C., Kaya, M., Chevalier, D., 2011. Fiber loop ringdown DNA and bacteria sensors. J. Biomed. Opt. 16 (5) 050501-1-3.

He, Z.H., Tian, F., Zhu, Y.N., Lavlinskaia, N., Du, H., 2011. Long-period gratings in photonic crystal fiber as an optofluidic label-free biosensor. Biosens. Bioelectron. 26, 4774–4778.

Kleinjung, F., Bier, F.F., Warsinke, A., Scheller, F.W., 1997. Fibre-optic genosensor for specific determination of femtomolar DNA oligomers. Anal. Chim. Acta. 350 (1–2), 51–58.

Long, F., Wu, S.X., He, M., Tong, T.Z., Shi, H.C., 2011. Ultrasensitive quantum dots-based DNA detection and hybridization kinetics analysis with evanescent wave biosensing platform. Biosens. Bioelectron. 26, 2390–2395.

Leung, A., Shankar, P.M., Mutharasan, R., 2008. Label-free detection of DNA hybridization using gold-coated tapered fiber optic biosensors (TFOBS) in a flow cell at 1310 nm and 1550 nm. Sens. Actuators B: Chem. 131, 640–645.

Liu, Y., Chen, S.M., Liu, Q., Peng, W., 2015. Micro-capillary-based evanescent field biosensor for sensitive, label-free DNA detection. Opt. Express 23 (16), 20686–20695.

Muller, W., Crothers, D.M., 1975. Interactions of heteroaromatic compounds with nucleic acids. Eur. J. Biochem. 54, 267–277.

Rindorf, L., Jensen, J.B., 2006. Photonic crystal fiber long-period gratings for biochemical sensing. Opt. Express 14 (18), 8224–8231.

Schmidt, P.M., Lehmann, C., Matthes, E., Bier, F.F., 2002. Detection of activity of telomerase in tumor cells using fiber optical biosensors. Biosens. Bioelectron. 17 (11–12), 1081–1087.

Sun, D.D., Guo, T., Ran, Y., Huang, Y.Y., Guan In-situ, B.O., 2014. DNA hybridization detection with a reflective microfiber grating biosensor. Biosens. Bioelectron. 61, 541–546.

Viphavakit, C., Komodromos, M., Themistos, C., Mohammed, W.S., Kalli, K., Rahman, B.M.A., 2015. Optimization of a horizontal slot waveguide biosensor to detect DNA hybridization. Appl. Opt. 54 (15), 4881–4888.

Verma, R., Gupta, B.D., 2013. Fiber optic SPR sensor for the detection of 3-pyridinecarboxamide (vitamin B3) using molecularly imprinted hydrogel. Sens. Actuators B: Chem. 177, 279–285.